2.5: Third-Order Nonlinear Spectroscopy

Now let's look at examples of diagrammatic perturbation theory applied to third-order nonlinear spectroscopy. Third-order nonlinearities describe the majority of coherent nonlinear experiments that are used including pump-probe experiments, transient gratings, photon echoes, coherent anti-Stokes Raman spectroscopy (CARS), and degenerate four wave mixing (4WM). These experiments are described by some or all of the eight correlation functions contributing to $R^{(3)}$:

$$R^{(3)} = \left(\frac{i}{\hbar}\right)^3 \sum_{\alpha=1}^{4} [R_\alpha - R_\alpha^*] \tag{2.5.1}$$

The diagrams and corresponding response first requires that we specify the system eigenstates. The simplest case, which allows us discuss a number of examples of third-order spectroscopy is a two-level system. Let's write out the diagrams and correlation functions for a two-level system starting in ρ_{aa}, where the dipole operator couples $|b\rangle$ and $|a\rangle$.

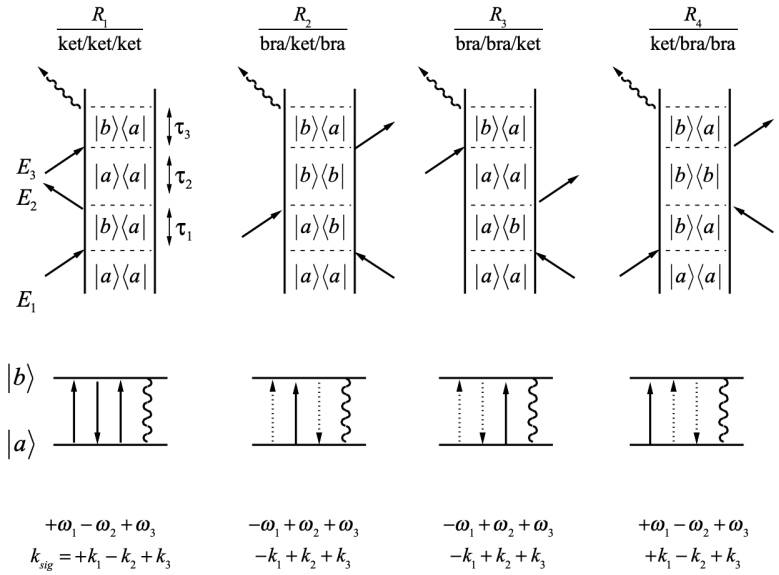

As an example, let's write out the correlation function for R_2 obtained from the diagram above. This term is important for understanding photon echo experiments and contributes to pump-probe and degenerate four-wave mixing experiments.

$$\begin{aligned} R_2 &= (-1)^2 p_a \left(\mu_{ba}^*\right) \left[e^{-i\omega_{ab}\tau_1 - \Gamma_{ab}\tau_1}\right] (\mu_{ba}) \left(e^{-i\omega_{bb}\tau_2 - \Gamma_{bb}\tau_2}\right) \left(\mu_{ab}^*\right) \left[e^{-i\omega_{ba}\tau_3 - \Gamma_{ba}\tau_3}\right] (\mu_{ab}) \\ &= p_a |\mu_{ab}|^4 \exp[-i\omega_{ba}(\tau_3 - \tau_1) - \Gamma_{ba}(\tau_1 + \tau_3) - \Gamma_{bb}(\tau_2)] \end{aligned}$$

The diagrams show how the input field contributions dictate the signal field frequency and wavevector. Recognizing the dependence of $E_{sig}^{(3)} \sim P^{(3)} \sim R_2(E_1 E_2 E_3)$, these are obtained from the product of the incident field contributions

$$\begin{aligned} \bar{E}_1 \bar{E}_2 \bar{E}_3 &= \left(E_1^* e^{+i\omega_1 t - i\bar{k}_1 \cdot \bar{r}}\right) \left(E_2 e^{-i\omega_2 t + i\bar{k}_2 \cdot r}\right) \left(E_3 e^{+i\omega_3 t - i\bar{k}_3 \cdot \bar{r}_3}\right) \\ &\Longrightarrow E_1^* E_2 E_3 e^{-\omega_{sig} t + i\bar{k}_{sig} \cdot \bar{r}} \\ \therefore \omega_{sig2} &= -\omega_1 + \omega_2 + \omega_3 \\ k_{sig2} &= -\bar{k}_1 + \bar{k}_2 + \bar{k}_3 \end{aligned}$$

Now, let's compare this to the response obtained from R_4. These we obtain

$$R_4 = p_a |\mu_{ab}|^4 exp\left[-i\omega_{ba}(\tau_3 + \tau_1) - \Gamma_{ba}(\tau_1 + \tau_3) - \Gamma_{bb}(\tau_2)\right] \tag{2.5.2}$$

$$\begin{aligned} \omega_{sig4} &= +\omega_1 - \omega_2 + \omega_3 \\ k_{sig4} &= +\bar{k}_1 - \bar{k}_2 + \bar{k}_3 \end{aligned}$$

Note that R_2 and R_4 terms are identical, except for the phase acquired during the initial period: $exp[i\phi] = exp[\pm i\omega_{ba}\tau_1]$. The R_2 term evolves in conjugate coherences during the τ_1 and τ_3 periods, whereas the R_4 term evolves in the same coherence state during both periods:

	Coherences in τ_1 and τ_3	Phase acquired in τ_1 and τ_3
R_4	$\|b\rangle\langle a\| \rightarrow \|b\rangle\langle a\|$	$e^{-i\omega_{ba}(\tau_1+\tau_3)}$
R_2	$\|a\rangle\langle b\| \rightarrow \|b\rangle\langle a\|$	$e^{-i\omega_{ba}(\tau_1-\tau_3)}$

The R_2 term has the property of time-reversal: the phase acquired during τ_1 is reversed in τ_3. For that reason the term is called "rephasing." Rephasing signals are selected in photon echo experiments and are used to distinguish line broadening mechanisms and study spectral diffusion. For R_4, the phase acquired continuously in τ_1 and τ_3, and this term is called "nonrephasing." Analysis of R_1 and R_3 reveals that these terms are non-rephasing and rephasing, respectively.

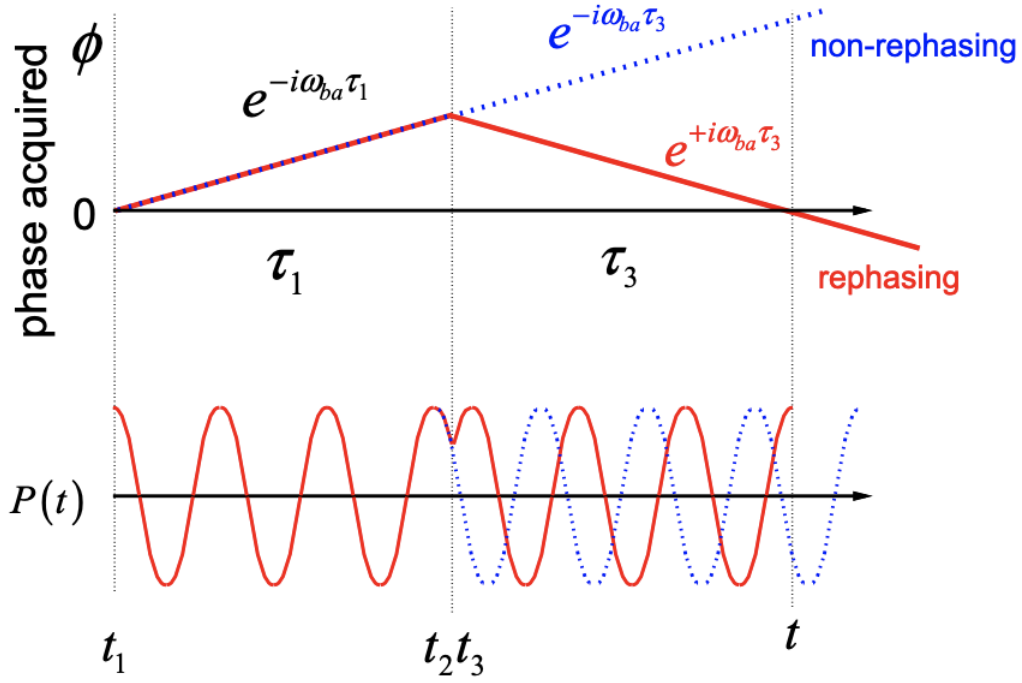

For the present case of a third-order spectroscopy applied to a two-level system, we observe that the two rephasing functions R_2 and R_3 have the same emission frequency and wavevector, and would therefore both contribute equally to a given detection geometry. The two terms differ in which population state they propagate during the τ_2 variable. Similarly, the non-rephasing functions R_1 and R_4 each have the same emission frequency and wavevector, but differ by the τ_2 population. For transitions between more than two system states, these terms could be separated by frequency or wavevector (see appendix). Since the rephasing pair R_2 and R_3 both contribute equally to a signal scattered in the $-k_1 + k_2 + k_3$ direction, they are also referred to as S_I. The nonrephasing pair R1 and R4 both scatter in the $+ k_1 - k_2 + k_3$ direction and are labeled as S_{II}.

Our findings for the four independent correlation functions are summarized below.

			ω_{sig}	k_{sig}	τ_2 population
S_I	rephasing	R_2	$-\omega_1+\omega_2+\omega_3$	$-k_1+k_2+k_3$	excited state
		R_3	$-\omega_1+\omega_2+\omega_3$	$-k_1+k_2+k_3$	ground state
S_{II}	non-rephasing	R_1	$+\omega_1-\omega_2+\omega_3$	$+k_1-k_2+k_3$	ground state
		R4	$+\omega_1-\omega_2+\omega_3$	$+k_1-k_2+k_3$	excited state